Structure and function of the cytochrome bc_1 complex of mitochondria and photosynthetic bacteria

Antony R Crofts* and Edward A Berry†

Progress has recently been made in the understanding of the function of the cytochrome bc_1 complex and related proteins in the context of recent structural information. The structures support many features that were predicted from sequence analysis and biophysical studies, but contain some surprises. Most dramatically, it is apparent that the iron–sulfur protein can take up different positions in different crystals, suggesting a novel mechanism for electron transfer through domain movement. Evidence from studies of mutant strains, in which the function of the sites or the binding of inhibitors is perturbed, has provided clues about the mechanism.

Addresses
*Center for Biophysics and Computational Biology and Department of Microbiology, University of Illinois at Urbana-Champaign, 388 Morrill Hall, 505 South Goodwin, Urbana, IL 61801, USA; e-mail: a-crofts@uiuc.edu
†Ernest Orlando Lawrence Berkeley National Laboratory, Mailstop 3-520, 1 Cyclotron Road, Berkeley, CA 94720, and University of California, Calvin Laboratory # 5230, Berkeley, CA 94720-5230, USA; e-mail: EABerry@lbl.gov

Current Opinion in Structural Biology 1998, 8:501–509

http://biomednet.com/elecref/0959440X00800501

Abbreviations

b_6f complex	plastohydroquinone:plastocyanin oxidoreductase
bc_1 complex	ubihydroquinone:cytochrome c oxidoreductase
b_H	higher potential cyt b heme
b_L	lower potential cyt b heme
cyt	cytochrome
E_m	redox midpoint potential
ISP	iron–sulfur protein
Q	ubiquinone or quinone
QH_2	ubihydroquinone or quinol
Q_i-site	quinone-reducing site
Q_o-site	quinol-oxidizing site

Introduction

The ubihydroquinone:cytochrome c oxidoreductases (bc_1 complexes) and the related plastohydroquinone:plastocyanin oxidoreductase (b_6f complexes) of oxygenic photosynthesis are the central components of all major energy-transducing respiratory and photosynthetic chains. They carry a flux that is several orders of magnitude greater than all anthropogenic energy usage. Two structures of the dimeric bc_1 complex from mitochondria have previously been published [1••,2••]. Reports from these and other groups suggest that solutions of additional structures are well advanced. An 8 Å structure of the chloroplast b_6f complex has been obtained using electron microscopy of thin three-dimensional crystals [3]. In addition, a number of partial structures have been solved, including soluble fragments of the Rieske-type iron–sulfur protein (ISP) from bovine mitochondrial bc_1 complexes [4] and the ISP [5] and cytochrome (cyt) f from chloroplast b_6f complexes [6,7].

General overview

The structure of the homodimeric bc_1 complex from chicken heart mitochondria [2••] is shown in Figure 1. The structure is similar to that of the bovine complex previously published [1••]. In the following discussion, we will focus on the chicken complex since the coordinates are available, but note that, except where otherwise indicated, the bovine structure of Xia *et al.* [1••] is essentially the same, as judged from the published figures. The protein extends 79 Å from the membrane into the matrix space and 31 Å into the intermembrane space, with a transmembrane region that is 40 Å thick, giving a total length of 150 Å perpendicular to the membrane. There are five main differences between the two structures (subunit numbering in parentheses in Roman numerals):

1. In the structure of Zhang *et al.* [2••], the ISP (V) and cyt c_1 (IV) subunits in the P-phase aqueous domain (intermembrane space) are complete. Disorder in the Xia *et al.* structure [1••] prevented the authors from assigning structures for ISP and most of cyt c_1 in the extrinsic domain. In the former structure, the extrinsic domain of the ISP from the Iwata *et al.* structure [4] was fit into the electron density. The work of Zhang *et al.* [2••] is the first published structure for a cyt c_1 subunit; the extrinsic domain comprises a fold with many features in common with Ambler's class I c cytochromes, but it has substantial additional protein in extra loops.

2. The positions of the Fe_2S_2 centers differ in the native complexes, which we will discuss more extensively below.

3. The chicken complex lacks subunit XI, but has well-resolved structures for subunits I–VIII and X. Subunit IX was not resolved in either structure.

4. The sequence of subunits other than cyt b (II) are not yet available for the chicken complex and the assignment of sidechains was therefore based on the bovine sequence. As there is a high degree of sequence homology among mitochondrial complexes, however, it is not expected that major differences will be found in critical regions.

5. The assignment of ligands to the propionates of the higher potential cyt b heme (b_H) is different in the two structures.

In addition to the chicken complex, the group at Berkeley has also solved structures for complexes from rabbit and

Figure 1

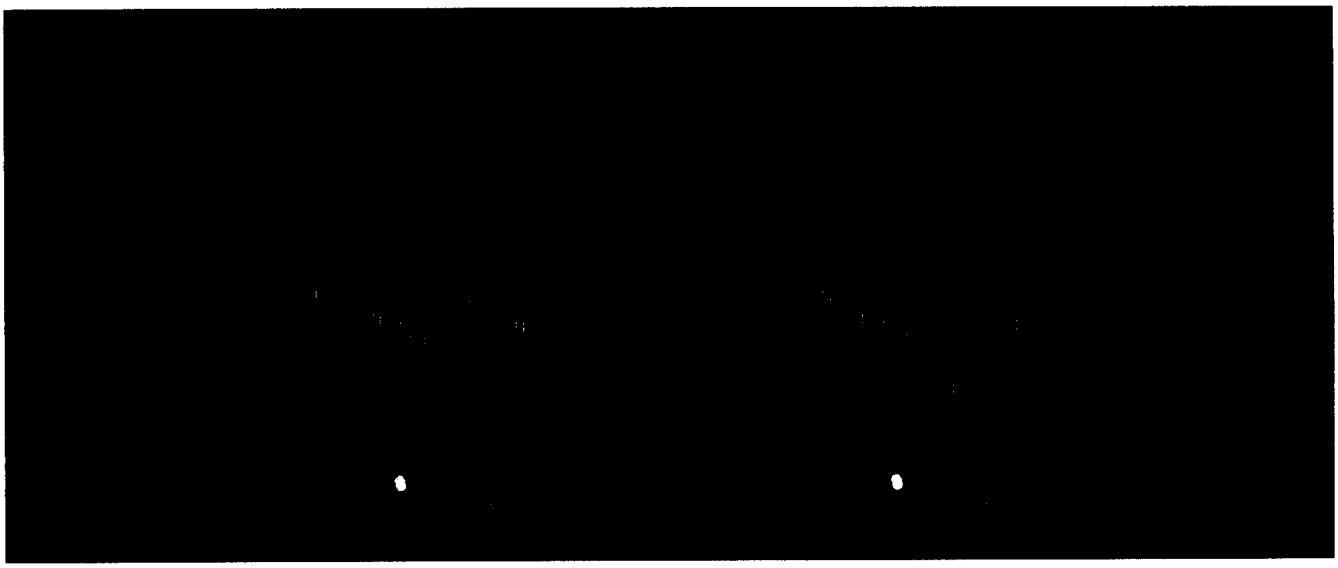

The chicken heart mitochondrial bc_1 complex. The homodimeric complex is shown as a stereopair for crossed-eye viewing, with the main part of the protein as a backbone model, colored by chain. The three catalytic subunits of the operational unit are shown highlighted as cartoon structures. The ISP (yellow ribbon), with its anchoring tail in one monomer, interacts with cyt b (blue ribbon) and cyt c_1 (red ribbon) in the other monomer. Other subunits are indicated by Roman numerals. Redox active prosthetic groups in the operational unit are shown as spacefilling models, with hemes b_H and b_L of cyt b in cyan, the quinone at the Q_i-site (Q_i) in green, heme c_1 in orange and the Fe_2S_2 (FeS) center in white. Electron density tentatively assigned to detergent or lipid molecules has been modeled as phosphatidylethanolamine (PEA), β-octylglucoside (BOG) and unknown (UNK) and are shown as red spacefilling models (in the unhighlighted monomer only, for clarity). The coordinates are from PDB file accession code 1bcc.

two different crystal forms of bovine heart mitochondrial bc_1 at a slightly lower resolution [2••].

The structures were solved with either inhibitors or substrates bound at the quinone-processing sites, allowing the identification of the catalytic interfaces [1••,2••]. The quinol-oxidizing site (Q_o-site) of the complex has a bifurcated volume, with domains proximal and distal to the heme b_H. Two different classes of inhibitors bind differentially in the two domains, suggesting that the occupancy of these domains by intermediates of the oxidation reaction might be important in catalysis. Weak density in the native structure of Zhang *et al.* [2••] might represent a quinone that is loosely bound at the Q_o-site. At the quinone-reducing site (Q_i-site), both groups report structures with bound antimycin and also provide evidence for occupancy by quinone in the native structures.

Four additional higher resolution structures of water-soluble fragments of extrinsic subunits (generated by proteolysis or specific mutagenesis) provide additional information. The structure of the extrinsic domain of cyt f, the analogue of cyt c_1 in the b_6f complex, has been solved for the b_6f complex from a higher plant [6] and from *Chlamydomonas reinhartii* [7]. The chloroplast protein shows no obvious homology, either in sequence or structure, to the mitochondrial protein. The structures of the extrinsic domains of the ISP from bovine mitochondria [4] and higher plant chloroplasts [5] have been reported. The domain that binds the metal center is highly conserved, but significant differences between the two structures were observed in the rest of the protein.

For a further discussion of these structures, the reader is referred to the original publications. In the remainder of this review, we will concentrate on the catalytic subunits of one monomer and also review mechanistic aspects. Figure 2a shows the subunits in outline, with the redox centers in place and the reactions of the modified Q-cycle superimposed.

The modified Q-cycle

The mitochondrial and purple bacterial bc_1 complexes catalyze the oxidation of ubiquinol and the reduction of cyt c through a modified Q-cycle [8–10]. Three catalytic subunits — a cyt b with two hemes, cyt c_1 and an ISP — house the mechanism. Two separate internal electron-transfer chains connect the three catalytic sites that catalyze the oxidation and reduction of the quinone pool and reduction of cyt c. The high-potential chain (Fe_2S_2 to cyt c_1), which receives the first electron, connects the Q_o-site to the acceptor, oxidized cyt c (or cyt c_2 in bacteria). A low-potential chain, consisting of the hemes of cyt b, transfers the second electron from a semiquinone at the Q_o-site to the Q_i-site. The kinetics of turnover have been resolved in photosynthetic bacteria, in which photoactivation allows good time resolution [9,11–16,17•]. The reactions of quinol oxidation are second order, rate determining (~600 μs at

Figure 2

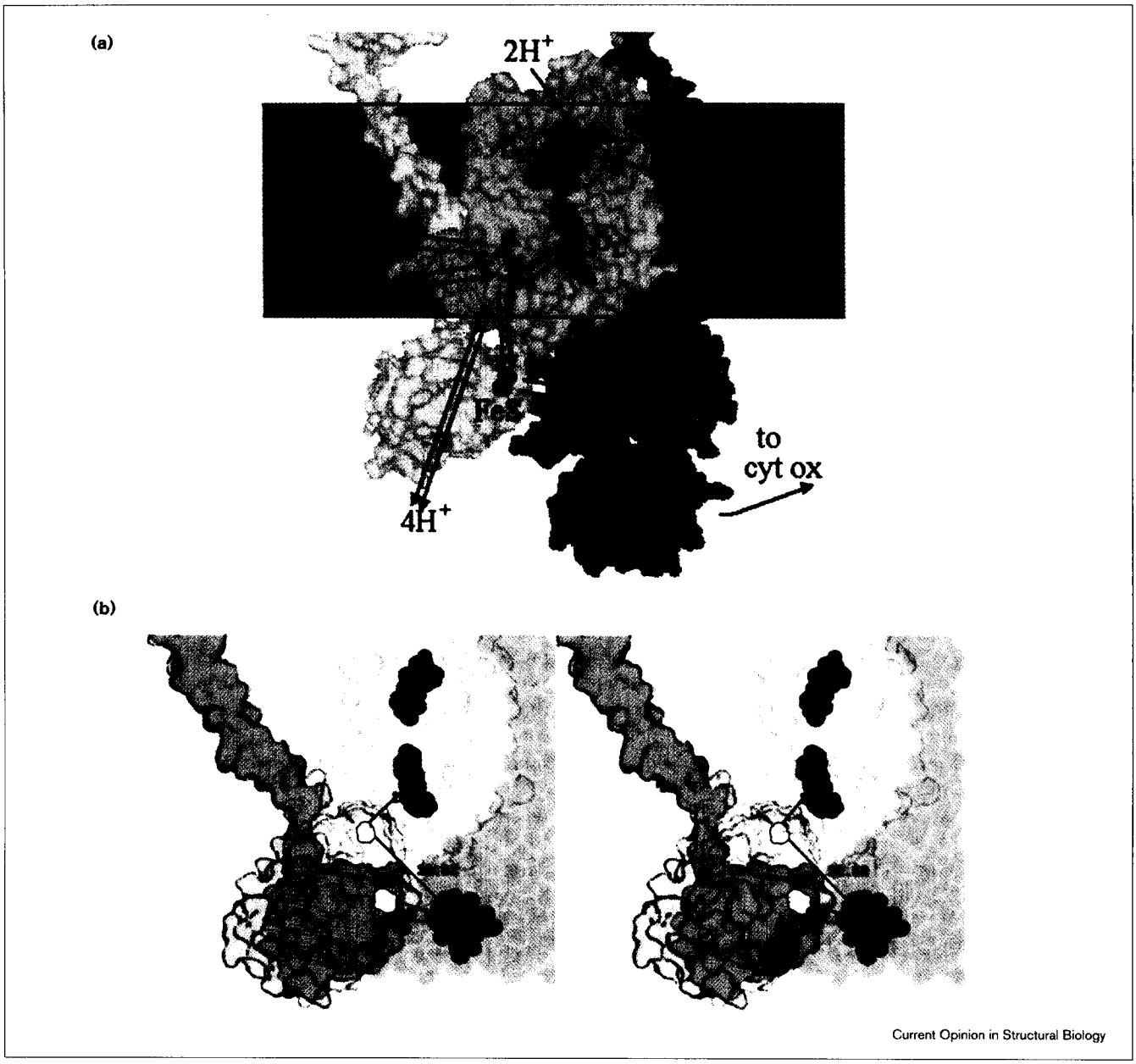

The catalytic core of the bc_1 complex. **(a)** The three subunits of the operational unit are shown as transparent surfaces, with cyt b in cyan, cyt c_1 in green and ISP in yellow. The metal centers are shown as spacefilling structures, with the cyt b hemes in blue, heme c_1 in green and the Fe_2S_2 center (FeS) in orange. Wireframe models of antimycin (brown) and stigmatellin (light green) indicate the Q_i and Q_o-sites, respectively. Docking with cyt c is represented with yeast cyt c as a pink transparent surface, with the heme in red. The model is based on the electron densities in a co-crystal of yeast cyt c with the bc_1 complex. The occupancy for cyt c was low because crystal contacts limited it to an interaction with only one monomer. The position of the heme iron is accurate, although the rest of the model is a preliminary fit of the yeast structure to the electron density. Superimposed on the structural model is a schematic representation of the reactions of the modified Q-cycle (see text for explanation). Electron transfers are blue arrows, proton transfers are red arrows, the binding or unbinding of quinone (Q) and quinol (QH_2) is represented by green arrows and the diffusion of cyt c is a black arrow. The shaded area is the hydrophobic phase. Coordinates are from the PDB file 3bcc. **(b)** The two positions of the ISP in the chicken complex (stereopair for crossed-eye viewing). The catalytic subunits are shown by their surfaces, with the metal centers as spacefilling models. Cyt b is in white and cyt c_1 is in red. The ISP in the stigmatellin-induced position is shown in yellow and the native position is in blue; where the configurations overlap, the ISP is green. The Fe_2S_2 centers are shown in white. Also shown are the positions of the center of density of the Fe_2S_2 irons in the bovine hexagonal (cyan), rabbit (magenta) and bovine $P2_1$ (green) crystals. The numbers shown by the lines indicate the distance (Å) from the nearest iron (or the center of density) of the Fe_2S_2 center to the iron of heme c_1 (in red) and heme b_L(in blue). Distances are shown for the two chicken Fe_2S_2 structures and the bovine hexagonal crystals; the latter position is thought to reflect the configuration for electron transfer. Coordinates from PDB files 1bcc and 3bcc. cyt ox, cytochrome c oxidase.

saturating quinol [QH_2]) and have a relatively high activation barrier. Electron transfer rate constants between Fe_2S_2 and cyt c_1 (<15 μs) and through the cyt b heme chain (<60 μs) cannot be resolved, but are estimated to be rapid. Similarly, electron transfer to the acceptor at the Q_i-site is more rapid than the rate-determining step and also cannot be resolved. Electron transfer across the membrane and the coupling of these redox reactions to the release or uptake of protons allows the complex to generate the transmembrane proton gradient that drives ATP synthesis.

Details of the mechanism at each Q-site are controversial. As an extension of the simple model [9,11], Ding, Dutton and co-workers have suggested a double-occupancy mechanism for quinol oxidation [13–16, 17•]. A continuing paradox is the mechanism by which the two electrons from quinol are funneled into separate chains. Various gating mechanisms have been proposed [13,18•,19•], including an interesting suggestion from Link [19•]. Based on the reaction center stigmatellin model [20], Link suggests that the semiquinone forms a complex with the reduced ISP that is only broken upon transfer of the second electron to the lower potential cyt b heme ($b_{L'}$). The activation barrier is under study in several laboratories and its nature is controversial. There are five main candidates: the movement of the ISP; the first deprotonation step [18•]; ligation or movement of the semiquinone [19•,21•]; the second deprotonation [21•]; and the low stability of the semiquinone [11]. As the structural evidence indicates an unsuspected dynamic complexity, these possibilities are not mutually exclusive. At the Q_i-site, the main bones of contention are the mechanism of formation of the cyt b-150 species (a form of cyt b_H that is associated with interactions between the heme b_H and semiquinone at the Q_i-site) and its relation to the stable semiquinone that is formed at the site [22–24].

Electron transfer by domain movement of the iron–sulfur protein

Even though the ISP was disordered, Xia *et al.* [1••] were able to locate the position of the Fe_2S_2 center in their crystals. Extrapolation of their distance data and a comparison with the position in the Zhang *et al.* native structure revealed substantial differences in the location of the center [2••,21•]. Subsequent work from the Berkeley group showed that the native structures for rabbit and cow (two crystal forms) had the center in a position similar to that of the chicken complex. When the chicken complex was co-crystallized with stigmatellin, a Q_o-site inhibitor, however, the ISP was found in a different position, with the Fe_2S_2 center located close to that calculated for the Xia *et al.* native structure [1••] (Figure 2b). Analysis of the structures and the distances between putative electron donors and acceptors showed that it was unlikely that a static structure with either configuration would be competent for all partial reactions of the complex. Zhang *et al.* [2••] therefore suggested that electron transfer during quinol oxidation must require domain movement of the extrinsic head of the ISP. The movement mainly involves a rotational displacement of ~57° (~65°), in which the head retains the same structure, the N-terminal membrane anchor is fixed and the action occurs in a short hinge region that undergoes extension. The conserved domain that binds the Fe_2S_2 center moves ~16.4 Å (21.2 Å) between a catalytic interface on cyt b, where the Fe_2S_2 center is reduced by quinol bound at the Q_o-site, and an interface on cyt c_1, where electron transfer to the heme occurs (values in parentheses refer to movement of the positions in bovine hexagonal crystals). This novel mechanism for rapid electron transfer across a distance is in contrast to the solid-state picture expected from the structures of other redox proteins [25]. We suggest that this mechanism may be of importance for determining how the two electrons from quinol enter different electron-transfer chains in the bifurcated reaction.

The ISP–cytochrome b interface and the architecture of the Q_o-site

The Zhang *et al.* structures show two important features of the reaction interface. The Q_o-site is a bifurcated pocket, with domains distal and proximal to heme $b_{L'}$. There is a channel to the lipid phase from the bifurcation point [21•]. In the structures with the ISP located near the cyt b, the distal domain opens to the ISP interface [1••,2••,21•]. The interface is provided by the conserved, concave surface of cyt b, into which the conserved Fe_2S_2-binding domain of the ISP fits tightly. In general, the spans in the sequence contributing to these structures are those predicted from sequence analysis and mutagenesis [26,27].

Interactions between the occupant of the Q_o-site and the ISP are detected by the effect on the electron paramagnetic resonance (EPR) spectrum of the reduced Fe_2S_2 center and also by the redox midpoint potential (E_m) [13–16,17•,28–32]. Several inhibitors bind more strongly to the reduced rather than the oxidized form and shift the E_m. Quinone (Q) also interacts with the reduced ISP to generate a new peak in the EPR spectrum centred at $g_x = 1.800$, which is lost upon reduction or extraction of the quinone and on the addition of inhibitors [13–16,17•, 31,32]. The occupant of the site may also perturb the spectrum of heme $b_{L'}$. The differential effects of inhibitors on the Fe_2S_2 center have provided the main basis for recognizing two classes of Q_o-site inhibitors. One such class contains 5-*n*-undecyl-6-hydroxy-4,7-dioxobenzothiazol (UHDBT), 3-*n*-undecyl-2-hydroxy-1,4-naphthoquinone (UHNQ), stigmatellin, and funiculosin (in yeast), which interact with the center and prevent electron transfer to cyt c_1. The second class comprises myxothiazol, mucidin, β-methoxyacrylate (MOA)–stilbene and similar compounds, which do not perturb the center or prevent electron transfer to cyt c_1, but instead inhibit turnover.

Both classes of inhibitor block quinol oxidation and are presumed to bind at the Q_o-site as analogues of quinol or its intermediates. Biochemical evidence has shown that

occupation of the Q_o-site is exclusive, so that inhibitors of one class will displace those of the other [29,30].

Similar features from both mitochondrial bc_1 structures [1••,2••] provide an explanation for these observations. Inhibitors of the first class have their rings in the Q_o-site distal domain, whereas those of the second class have their pharmacophore groups in the proximal domain. The 'tails' occupy an overlapping volume and extend from the site into the lipid through a channel with a cross section that is comparable to that of the tail. At the distal domain, the carbonyl and methoxy oxygens of the stigmatellin ring can be modeled as being within hydrogen-bonding distance of Nε of His161 of the ISP. His161 is a ligand to the Fe_2S_2 center and probably mimics the quinol:oxidized–ISP reaction intermediate [19•,20,21•]. The configuration of the inhibitors in the proximal domain is less certain. Structures from the Berkeley group that contain iodinated MOA–stilbene-type inhibitors clearly show the orientation of the pharmacophore with respect to the two rings as reaching into the proximal domain towards heme b_L.

Mutations that affect interaction with the occupant

The extensive literature on mutations of cyt b has been nicely summarized by Brasseur *et al.* [33]. The most useful data on interactions with the ISP come from a set of papers from Ding, Dutton and colleagues [13–16,17•], in which they explore the g_x = 1.800 signal as a function of the state of the quinone occupant within a series of mutant strains. This set has been supplemented by our own studies in collaboration with the group [21•,24]. The results show three broad classes of effect:

1. Sites at which mutation prevented the formation of the g_x = 1.800 signal and blocked electron transfer.

2. Sites at which mutation prevented the formation of the g_x signal, but allowed an inhibited rate of electron transfer.

3. Sites at which mutation did not prevent formation of the g_x signal, but blocked electron transfer.

Most sites at which mutations generate resistance to stigmatellin, but not myxothiazol, are among those in classes 1 and 2. The majority of sites at which mutations generate resistance to myxothiazol, but not stigmatellin, fall into class 3.

This somewhat simplistic grouping reflects an underlying pattern seen on the analysis of the locations of the residues at which mutation leads to resistance to Q_o-site inhibitors or modified function in the structure [21•]. Residues in groups 1 and 2 impinge either on the distal domain, where stigmatellin binds, or on the interface on cyt b at which the ISP docks. Their effects on the g_x signal and electron transfer probably reflect the need for the correct binding of both ISP and quinone; if either one is impeded, the formation of either the g_x = 1.800 complex or the reaction complex of quinol and the oxidized ISP will be less probable. Mutations of residues in the ISP that impinge on the interface [34–37] also lead to an inhibited turnover, presumably through this same effect (Figure 3a).

In contrast, residues in group 3 cluster around the proximal domain and provide most of its surface. This disposition can be seen in Figure 3b, in which the residues are color coded according to the above grouping. Since the mutations of this latter group do not prevent binding in the distal domain but do inhibit turnover, we have suggested that their inhibitory effect must reflect a need for the occupancy of this domain by a reaction intermediate. Two mechanisms seem plausible. One is a variant of the double-occupancy model of Ding, Dutton and co-workers [13–16,17•]. The other is a single-occupancy mechanism, in which the semiquinone intermediate moves to the proximal domain from the distal domain where it is formed upon the reduction of Fe_2S_2, before electron transfer to heme b_L and the formation of the product quinone [21•].

We prefer the latter explanation, since the structures from neither group show evidence of the tightly bound quinone expected from the double-occupancy model and the protein would have to undergo considerable displacement in order to accommodate two quinones. An in-site movement of the occupant upon formation of the semiquinone has been demonstrated in reaction centers [20,38]. Such a movement at the Q_o-site could resolve the paradox of the bifurcated reaction, since the reaction partners for the decoupling reaction would be separated, and it could perhaps also contribute to the activation barrier [21•].

The Q_i-site

The spans contributing to the Q_i-site [1••,2••] are as expected from predictions based on sequence analysis and mutations affecting the site [26,27,33]. An unexpected feature is the positioning of helix E. The de-loop reaches over the site and the main part of helix E is on the other side of helix A. The N-terminal section, however, contributes to the site as expected. Both groups report structures with antimycin bound to the Q_i-site. The Berkeley group [2••] has modeled the density in the native structure as a quinone in a position similar to where density is lost upon binding antimycin, as previously reported by Xia *et al.* [1••]. In general, the two structures seem to be well in accord, although the Berkeley structure [2••] has a well-defined ligation between Arg101 and a propionate sidechain of the heme that was modeled differently in the Xia *et al.* structure [1••].

Mutagenesis studies and clues to the mechanism

The structures provide a new understanding of the large body of information on the effects of mutation on inhibitor binding and function (reviewed in [33]). The volume of the site is larger than needed to accommodate either the

Figure 3

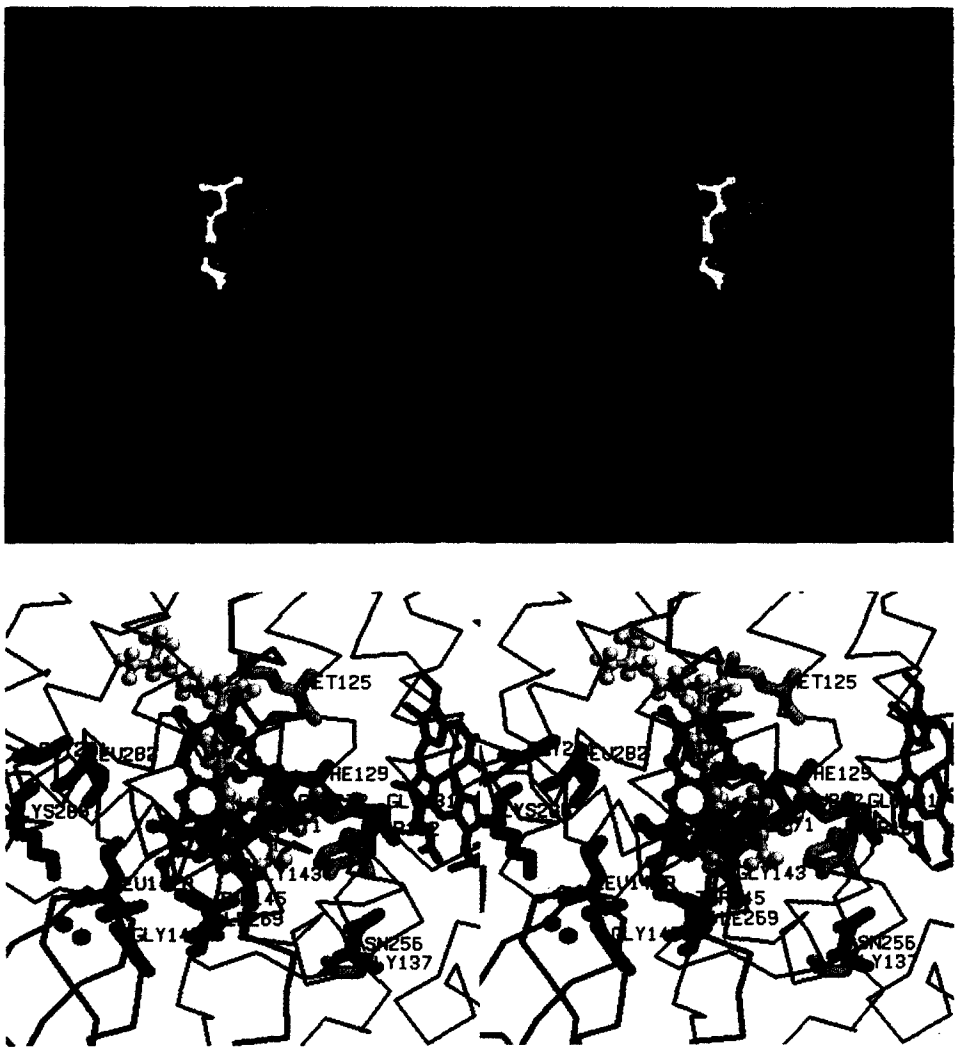

Details of the Q_o-site (stereopairs for crossed-eye viewing). **(a)** Residues on cytochrome b at the interface with ISP. The protein is shown as a backbone structure: cyt b, blue; ISP, green; cyt c_1, cyan, with residues at the interface highlighted. Spacefilling models are color coded according to their distance from the the nearest atom of the ISP: blue, within 5.0 Å; blue-green, within 4 Å; green, within 3.5 Å; and yellow, within 3.0 Å. Labeled residues are those whose mutation changes the $g_x = 1.800$ signal. The red ball-and-stick model indicates stigmatellin. The white model represents ISP residues whose mutagenesis interferes with the $g_x = 1.800$ signal. Coordinates from PDB file 2bcc. **(b)** Residues in the Q_o-site that modify function [13–16,17•,21•,24] color coded by their effect on the $g_x = 1.800$ signal and the turnover of the site. The ball-and-stick structures are myxothiazol in white and stigmatellin in light green. Residue sidechains are shown as stick models: yellow, normal occupancy of g_x and electron transfer inhibited (M125, E272, Y132 and G137); orange, changes to F129 have either yellow (to histidine, lysine or arginine), magenta (asparagine, isoleucine, glycine or leucine) or blue-green effects (valine); magenta, blocks formation of g_x and electron transfer blocked (G143, T145, L269 and L282); red, reduced formation of g_x and electron transfer slowed (K288 and G291); blue, mutations are either magenta (P271L) or blue-green (P271S); blue-green, g_x normal and moderate rate electron transfer (N256); brown or gray in ISP (chain R), affect formation of g_x (G142.R and L143.R). Heme b_L is shown as an orange stick model and atoms of Fe_2S_2 are small orange spheres. Coordinates from PDB file 2bcc modified by inclusion of a myxothiazol model to fit the electron density and energy minimization of residues within 6 Å of the model in order to fit the changed electron densities of the protein in the myxothiazol-containing structure.

substrate or antimycin. These two occupants are found in different, but overlapping volumes, with antimycin located deeper in the pocket and closer to heme b_H. It is modeled as forming several hydrogen bonds, which quinone does not. The sidechains at which mutations affect function impinge on these volumes differentially and supply clues as to the probable domains that are occupied by other inhibitors. Figure 4 shows the Q_i-site with quinone in position (the residues are coded according to inhibitor resistance). The different positions of antimycin and quinone, and the differential sensitivity of mutations at other residues, suggest that the intermediates might also move

Figure 4

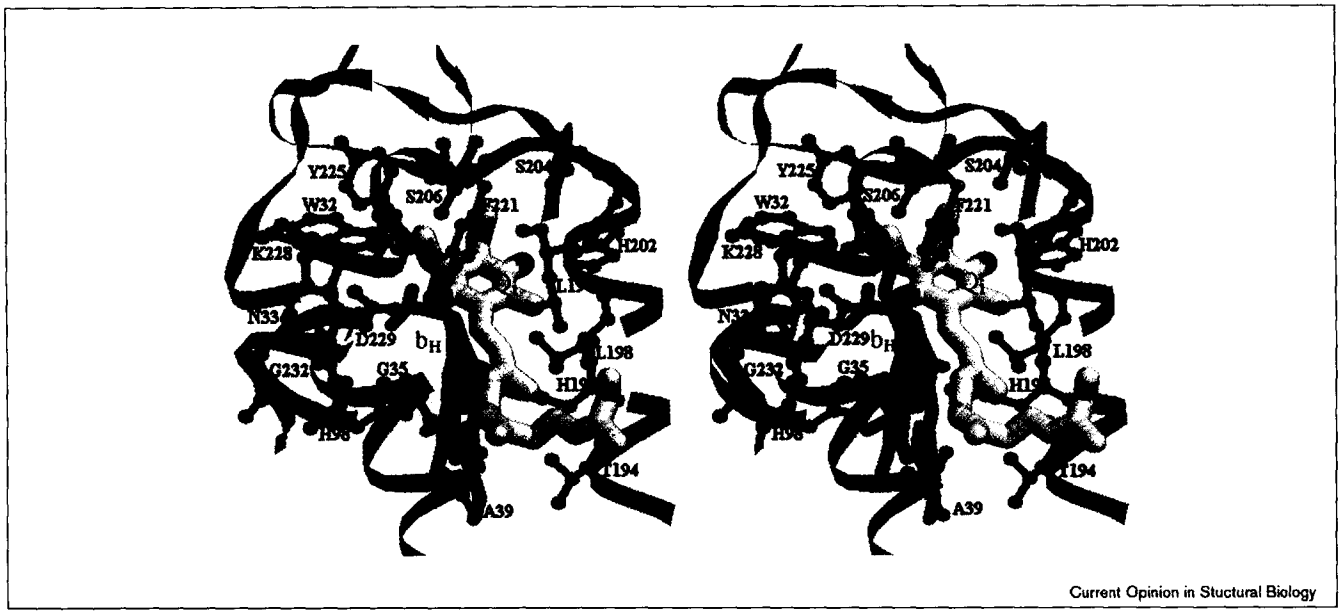

The Q_i-site (stereopair for crossed-eye viewing). Residues whose change gives rise to inhibitor resistance [33] are shown as ball-and-stick models coded according to the inhibitor: yellow, antimycin and diuron (N33); orange, diuron and HQNO (L19 and Y225); brown, HQNO and funiculosin (W32 and G35); green, funiculosin (T194 and L198); cyan, antimycin and funiculosin (A39 and F221) (also show diuron resistance); blue, antimycin (K228, D229 and G232). Heme b_H is shown as a magenta stick model, with the iron as a van der Waals' sphere in orange. The histidines – two heme ligands (H98 and H197) and H202, which is important for function, are in CPK coloring. A tentative model for quinone (Q_i) is shown as a fat stick model in CPK colors. Coordinates from PDB file 1bcc.

in the site during catalysis. We suggest that the inhibitors might occupy different positions, reflecting the binding domains of different intermediates; perhaps antimycin mimics the semiquinone and the hydrogen-bonding pattern of the inhibitor reflects the stabilization of the species characteristic of that site [22–24].

Proton processing

At both quinone-processing sites, the substrate-binding pockets are located close to the aqueous interfaces. They are connected to the external phase by obvious channels, indicated by the surface as mapped by a 1.4 Å radius probe. This suggests that water and protons have access to the sites and that special channels, such as those in the reaction centers [20,38], may not be needed.

The role of the dimer and minor subunits

Bacterial complexes only have the three catalytic subunits and sometimes an additional subunit, IV, which may be involved in the stabilization of the complex [39–41]. Subunits 1 and 2 of the mitochondrial complex have their origin in a protein import processing apparatus (see [42] for a review) and do not appear to be involved in catalysis [43]. The structures provide new insights into the role of the smaller subunits [1••,2••], which seem to have stabilizing interactions with other subunits and/or between monomers, but do not impinge on the catalytic interface. Subunit VII, however, has an interesting N-terminal finger that reaches over to the channel in cyt b, connecting the Q_i-site with the aqueous phase.

The dimeric structure appears to serve several functions. The ISP subunit interacts with both monomers. The mobile head travels between the catalytic interfaces on cyt b and cyt c_1 of one monomer. The N-terminal anchor is locked in a vice provided by both cyt b subunits and is also constrained by contacts with the transmembrane helices of cyt c_1 and subunits VII and X, and subunit I in the matrix phase of the other monomer.

Xia *et al.* [1••] suggested that communication between Q_o and Q_i-sites of opposite monomers might be facilitated by their access from a common cavity. Access from the cavity to the lipid phase is far wider than the channel into either site, so this is unlikely to be an essential pathway. Such a cavity may, however, favor transfer between sites by some constraint on local diffusion from the cavity.

Interactions between monomers occur through substantial interfaces between the core II, cyt b and c_1 subunits. The b_L hemes of the two monomers are 21 Å apart, allowing the possibility of rapid electron transfer between them. The authors are not aware of any kinetic evidence for such communication between dimers. Titrations with myxothiazol of the flash-induced reduction of cyt b_H in the presence of antimycin show no hint of the sigmoidal curve expected if

such electron transfer occurred (SJ Hong, J Fernandez-Velasco, AR Crofts, unpublished data).

Conclusions

The structure of this important enzyme has provided insights into their mechanism and has suggested novel mechanistic features. The two quinone-processing sites show some features that are similar to those known from earlier work in photochemical reaction centers, but there are no obvious structural motifs and there are some interesting differences in both structure and mechanism. The movement of the ISP indicates a novel mechanism for rapid electron transfer by domain movement. Future work will no doubt concentrate on understanding these mechanistic features in the context of the structure. In addition, the bc_1 complex is the site of action of several inhibitors that are of increasing agrochemical importance; the structures will provide an invaluable aid to understanding how these work. The Q_o-site of the complex is also one of the main sites of formation of the superoxide anion, leading to oxygen radicals that are thought to be a main cause of cell damage, aging and DNA damage. It seems likely that the design and mechanism of the site have evolved in order to minimize this unwanted side effect and the structures will provide new insights into how this works.

Note added in proof

A third structure for the beef heart mitochondrial complex has recently been published that includes two novel features [44]. Subunit IX is shown to be lodged between the two 'core' subunits, hinting at the mechanism of protein import processing and how mitochondrial targeting presequences are recognized. The ISP is found in a third position, an intermediate of the two positions found in the other published structures. The authors believe this is important in a 'three-state' gating mechanism for the bifurcated reaction.

Acknowledgements

We acknowledge with gratitude the support for this research provided by National Institutes of Health grants GM 35438 (to ARC) and DK 44842 (to EAB) and the Office of Health and Environmental Research, US Department of Energy, under contract DE-AC03-76SF00098 (EAB).

References and recommended reading

Papers of particular interest, published within the annual period of review, have been highlighted as:

- • of special interest
- •• of outstanding interest

1. •• Xia D, Yu C-A, Kim H, Xia J-Z, Kachurin AM, Zhang L, Yu L, Deisenhofer J: **Crystal structure of the cytochrome bc_1 complex from bovine heart mitochondria.** *Science* 1997, **277**:60-66.

This paper describes the first reported structure for the complete bc_1 complex at atomic resolution. The structure of the beef heart mitochondrial complex provides invaluable insights into the general features of the dimeric complex and reveals the location of the catalytic sites for quinone processing and the location of the heme groups. The structure showed a paradoxical position of the Fe_2S_2 center, which was too distant from cyt c_1 to allow the rapid rates of electron transfer observed.

2. •• Zhang Z, Huang L-S, Shulmeister VM, Chi Y-I, Kim K-K, Hung L-W, Crofts AR, Berry EA, Kim S-H: **Electron transfer by domain movement in cytochrome bc_1.** *Nature* 1998, **392**:677-684.

This paper describes the first structure of the complete bc_1 complex to have all the catalytic subunits defined at atomic resolution. In addition to showing the structure for cyt c_1, this paper showed the iron–sulfur protein (ISP) *in situ* and demonstrated that the extrinsic domain could occupy different positions in the complex. This provided evidence for a novel mechanism of electron transfer by domain movement of the ISP. The main subject matter is the chicken heart mitochondrial complex with and without inhibitors, but additional information on the structures of the rabbit complex and two different forms of the beef complex is also given, each with a different position for the ISP.

3. Mosser G, Breyton C, Olofsson A, Popot J-L, Rigaud J-L: **Projection map of cytochrome b_6f complex at 8 Å resolution.** *J Biol Chem* 1997, **272**:20263-20268.

4. Iwata S, Saynovits M, Link TA, Michel H: **Structure of a water soluble fragment of the 'Rieske' iron-sulfur protein of the bovine heart mitochondrial cytochrome bc_1 complex determined by MAD phasing at 1.5 Å resolution.** *Structure* 1996, **4**:567-579.

5. Carrell CJ, Zhang HM, Cramer WA, Smith JL: **Biological identity and diversity in photosyntheris and respiration – structure of the lumen-side of the chloroplast Rieske protein.** *Structure* 1998, **5**:1613-1625.

6. Martinez SE, Huang D, Szczepaniak A, Cramer WA, Smith JL: **Crystal structure of chloroplast cytochrome f reveals a novel cytochrome fold and unexpected heme ligation.** *Structure* 1994, **2**:95-105.

7. Berry EA, Huang L-S, Chi Y, Zhang Z, Malkin R, Fernandez-Velasco JG: **The crystallization and structure of a soluble form of *Chlamydomonas reinhartii* cytochrome f [abstract].** *Biophys J* 1997, **72**:A125.

8. Mitchell P: **Possible molecular mechanisms of the protonmotive function of cytochrome systems.** *J Theor Biol* 1976, **62**:327-367.

9. Crofts AR: **The mechanism of ubiquinol:cytochrome c oxidoreductases of mitochondria and of *Rhodopseudomonas sphaeroides*.** In *The Enzymes of Biological Membranes*. Edited by Martonosi AN. New York: Plenum Publishing Corporation; 1985:347-382.

10. Brandt U, Trumpower BL: **The protonmotive Q cycle in mitochondria and bacteria.** *Crit Rev Biochem* 1994, **29**:165-197.

11. Crofts AR, Wang Z: **How rapid are the internal reactions of the ubiquinol:cytochrome c_2 oxidoreductase?** *Photosynth Res* 1989, **22**:69-87.

12. Gennis RB, Barquera B, Hacker B, van Doren SR, Arnaud S, Crofts AR, Davidson E, Gray KA, Daldal F: **The bc_1 complexes of *Rhodobacter sphaeroides* and *Rhodobacter capsulatus*.** *J Bioenerg Biomembr* 1993, **25**:195-210.

13. Ding H, Robertson DE, Daldal F, Dutton PL: **Cytochrome bc_1 complex [2Fe-2S] cluster and its interaction with ubiquinone and ubihydroquinone at the Q_o site: a double-occupancy Q_o site model.** *Biochemistry* 1992, **31**:3144-3158.

14. Ding H, Moser CC, Robertson DE, Tokito MK, Daldal F, Dutton PL: **Ubiquinone pair in the Q_o site central to the primary energy conversion reactions of cytochrome bc_1 complex.** *Biochemistry* 1995, **34**:15979-15996.

15. Ding H, Daldal F, Dutton PL: **Ion pair formation between basic residues at 144 of the cyt b polypeptide and the ubiquinones at the Q_o site of the cyt bc_1 complex.** *Biochemistry* 1995, **34**:15997-16003.

16. Saribas S, Ding H, Dutton PL, Daldal F: **Tyrosine 147 of cytochrome b is required for efficient electron transfer at the ubihydroquinone oxidase site (Q_o) of the cytochrome bc_1 complex.** *Biochemistry* 1995, **34**:16004-16012.

17. • Saribas S, Ding H, Dutton PL, Daldal F: **Substitutions at position 146 of cytochrome b affect drastically the properties of heme b_L and the Q_o site of *Rhodobacter capsulatus* cytochrome bc_1 complex.** *Biochim Biophys Acta* 1997, **1319**:99-108.

This paper by Saribas *et al.* is the most recent of a series from the collaboration between the Dutton and Daldal laboratories (see also [13–16]), in which the properties of strains of *Rb. capsulatus* with mutations in the bc_1 complex that effect the Q_o-site have been explored. The effects of mutation on interactions of the Q_o-site occupant with the iron–sulfur protein, as shown by the electron paramagnetic resonance spectrum, have been interpreted in the context of the double occupancy of the site by two quinone species.

18. Brandt U: **Energy conservation by bifurcated electron-transfer in**
• **the cytochrome-bc_1 complex.** *Biochim Biophys Acta* 1996, **1275**:41-46.
Brandt provides an excellent overview of the bifurcated reaction and its paradoxical features. The author emphasizes the need for a gating mechanism to ensure that the two electrons from quinol pass down the separate high and low potential chains. He proposes a proton-gated charge-transfer mechanism for the reaction, which is controlled by the deprotonation of the substrate ubihydroquinone and involves double occupancy of the Q_o-site.

19. Link TA: **The role of the 'Rieske' iron sulfur protein in the**
• **hydroquinone oxidation (Q_p-) site of the cytochrome bc_1 complex: the 'proton-gated affinity change' mechanism.** *FEBS Lett* 1996, **412**:257-264.
The paper by Link provides an alternative perspective on the mechanism of the bifurcated reaction. Link emphasizes the properties of the reaction complex formed between quinol and the oxidized iron–sulfur protein (ISP) and the intermediate state formed after single electron transfer. He suggests that the gating of the bifurcated reaction occurs through the binding affinity between semiquinone and the reduced ISP, which would raise the potential of the ISP so as to prevent reaction with cyt c_1. Further reaction can occur only after electron transfer from the semiquinone to heme b_L.

20. Lancaster CR, Michel H: **The coupling of light-induced electron transfer and proton uptake as derived from crystal structures of reaction centers from *Rhodopseudomonas viridis* modified at the binding site of the secondary quinone, Q_B.** *Structure* 1997, **5**:1339-1359.

21. Crofts AR, Barquera B, Gennis RB, Kuras R, Guergova-Kuras M,
• Berry EA: **Mechanistic aspects of the Q_o-site of the bc_1 complex as revealed by mutagenesis studies, and the crystallographic structure.** In *The Phototrophic Prokaryotes.* Edited by Peschek GA, Loeffelhardt W, Schmetterer G: New York: Plenum Publishing Corporation; 1997:229–239.
The paper explores the structure of the chicken mitochondrial bc_1 complex in the context of information from mutant strains that affect turn over or inhibitor binding at the Q_o-site. As the bound quinone species expected at the site from the double-occupancy model is absent in the crystallographic structures, the authors explore alternative explanations for the phenotype of the mutant strains. They suggest that quinol oxidation proceeds from a reaction complex between quinol in the distal (from heme b_L) domain of the bifurcated site and the oxidized iron–sulfur protein, and that after single electron transfer, the semiquinone flips to the proximal domain before transferring an electron to heme b_L.

22. Robertson DE, Prince RC, Bowyer JR, Matsuura K, Dutton PL, Ohnishi T: **Thermodynamic properties of the semiquinone and its binding site in the ubiquinol:cytochrome c (c_2) oxidoreductase of respiratory and photosynthetic systems.** *J Biol Chem* 1984, **259**:1758-1763.

23. Rich PR, Jeal AE, Madgwick SA, Moody AJ: **Inhibitor effects on redox-linked protonations of the b hemes of the mitochondrial bc-1 complex.** *Biochim Biophys Acta* 1990, **1018**:29-40.

24. Crofts AR, Barquera B, Bechmann G, Guergova M, Salcedo-Hernandez R, Hacker B, Hong S, Gennis RB: **Structure and function in the bc_1-complex of *Rb. sphaeroides.*** In *Photosynthesis: from Light to Biosphere.* Edited by Mathis P. Dordrecht: Kluwer Academic Publishing; 1995:493-500.

25. Moser CC, Page CC, Farid R, Dutton PL: **Biological electron transfer.** *J Bioenerg Biomembr* 1995, **27**:263-274.

26. Crofts AR, Hacker B, Barquera B, Yun C-H, Gennis R: **Structure and function of the *bc*-complex of *Rhodobacter sphaeroides.*** *Biochim Biophys Acta* 1992, **1101**:162-165.

27. Degli Esposti M, De Vries S, Crimi M, Ghelli A, Patarnello T, Meyer A: **Mitochondrial cytochrome b: evolution and structure of the protein.** *Biochim Biophys Acta* 1993, **1143**:243-271.

28. Bowyer JR, Dutton PL, Prince RC, Crofts AR: **The role of the Rieske iron-sulfur center as the electron donor to ferricytochrome c_2 in *Rhodopseudomonas sphaeroides.*** *Biochim Biophys Acta* 1980, **592**:445-460.

29. Meinhardt SW, Crofts AR: **The site and mechanism of action of myxothiazol as an inhibitor of electron transfer in *Rhodopseudomonas sphaeroides.*** *FEBS Lett* 1982, **149**:217-222.

30. Link TA, Haase U, Brandt U, von Jagow G: **What information do inhibitors provide about the structure of the hydroquinone oxidation site of ubiquinol:cytochrome c oxidoreductase?** *J Bioenerg Biomembr* 1993, **25**:221-232.

31. Siedow JN, Power S, De La Rosa FF, Palmer G: **The preparation and characterization of highly purified, enzymically active complex III from baker's yeast.** *J Biol Chem* 1978, **253**:2392-2399.

32. De Vries S, Albracht SPJ, Berden JA, Slater EC: **The pathway of electrons through QH_2:cytochrome c oxidoreductase studied by pre-steady-state kinetics.** *Biochim Biophy Acta* 1982, **681**:41-53.

33. Brasseur G, Sami Saribas A, Daldal F: **A compilation of mutations located in the cytochrome b subunit of the bacterial and mitochondrial bc_1 complex.** *Biochim Biophys Acta* 1996, **1275**:61-69.

34. Gatti DL, Meinhardt SW, Ohnishi T, Tzagoloff A: **Structure and function of the mitochondrial bc_1 complex. A mutational analysis of the yeast Rieske iron-sulfur protein.** *J Mol Biol* 1989, **205**:421-435.

35. Van Doren SR, Gennis RB, Barquera B, Crofts AR: **Site-directed mutations of conserved residues of the Rieske iron-sulfur subunit of the cytochrome *bc_1* complex of *Rhodobacter sphaeroides* blocking or impairing quinol oxidation.** *Biochemistry* 1993, **32**:8083-8091.

36. Liebl U, Sled V, Brasseur G, Ohnishi T, Daldal F: **Conserved non liganding residues of *Rb. capsulatus* Rieske iron sulfur protein of the bc_1 complex are essential for protein structure, properties of the [2Fe2S] cluster and communication with the quinone pool.** *Biochemistry* 1993, **36**:11675-11684.

37. Brasseur G, Sled V, Liebl U, Ohnishi T, Daldal F: **The amino terminal portion of the Rieske iron sulfur protein contributes to the ubihydroquinone oxidation (Q_o) site catalysis on *Rb. capsulatus* bc_1 complex.** *Biochemistry* 1997, **36**:11685-11696.

38. Stowell MHB, McPhillips TM, Rees DC, Soltis SM, Abresch E, Feher G: **Light-induced structural changes in photosynthetic reaction center: implications for mechanism of electron-proton transfer.** *Science* 1997, **276**:812-815.

39. Chen YR, Yu C-A, Yu L: **Functional expression of subunit IV of *Rhodobacter sphaeroides* cytochrome bc_1 complex and reconstitution of recombinant protein with three-subunit core complex.** *J Biol Chem* 1996, **271**:2057-2062.

40. Mather MW, Yu L, Yu C-A: **The involvement of threonine 160 of cytochrome b of *Rhodobacter sphaeroides* cytochrome bc_1 complex and interaction with subunit IV.** *J Biol Chem* 1995, **270**:28668-28675.

41. Tso S-C, Sadoski R, Millett F, Yu C-A, Yu L: **Effect of subunit IV of *Rhodobacter sphaeroides* cytochrome bc_1 complex on electron transfer to cytochrome c.** *Biophys Soc Annu Meeting* 1998, abstract M-PM-05.

42. Whelan J, Glaser E: **Protein import into plant mitochondria.** *Plant Mol Biol* 1997, **33**:771-789.

43. DiRago JP, Sohm F, Boccia C, Dujardin G, Trumpower BL, Slonimski PP: **A point mutation in the mitochondrial cytochrome b gene obviates the requirement for the nuclear encoded core protein 2 subunit in the cytochrome bc_1 complex in *Saccharomyces cerevisiae.*** *J Biol Chem* 1997, **272**:4699-4704.

44. Iwata S, Lee JW, Okada K, Lee JK, Iwata M, Rasmussen B, Link TA, Ramaswamy S, Jap BK: **Complete structure of the 11-subunit bovine mitochondrial cytochrome bc_1 complex.** *Science* 1998, **281**:64-71.